

BCA Whitepaper: Seep Characterization



Seep Characterization Whitepaper V1.0

Beaver Creek Analytical, LLC

Original Author: Ryan Bell, PhD

Original Date: February 2025

Changelog:

Date	Version	Comment
Feb, 2025	V1.0	Initial Release

Seep Characterization

Researchers aim to perform chemical characterization of seep sites because compositional and isotopic ratios can provide insights into the nature of the seeps' source reservoir^{1,2}. However, directly accessing seep sites for chemical analysis can be challenging and costly. There are excellent examples of researchers employing effective techniques to track down seep sources with *in situ*, real-time chemical data, which provides a reasonable approach³. Nevertheless, to maximize efficiency and minimize ship time and related expenses, a multifaceted approach should be adopted. Remote techniques such as satellite sheen detection, acoustic sensing for bubbles or seafloor anomalies, and seismic and magnetic sensing can each contribute to a regional search for likely seeps locations in a more cost-effective and reliable manner. After identifying areas of interest, specific sites can be approached with a mobile platform (AUV, ROV, tow-platform, lander, etc.) using real-time sonar and a suite of *in situ* sensors to inform search decision-making. A mobile platform for *in situ* analysis and sensor-triggered sampler designed for tracking plume extent is shown in Figure 1.



Figure 1. Towed platform used for mapping plume extents of the Deepwater Horizon oil-spill shown with a sensor suite (UMS included) and Niskin Samplers.

When approaching subsea seeps, it is essential to have a comprehensive suite of sensors to ensure researchers the best chance of success. The expense of such equipment is generally inconsequential compared to costs associated with ship-related activities. Equipped with an underwater mass spectrometer (UMS), which offers excellent detection limits ($3\sigma < 30$ nM) and response times ($T_{90} < 30$ s), methane from seep emissions can be detected at considerable distances, even hundreds of meters away, despite strong variability in emission patterns⁴⁻⁷ (Figure 2). Depending on several factors such as bubble composition, emission rate, and depth, ethane may also be detectable far from the source of a seep plume. Additionally, effective acoustic sonar units can positively locate bubble signatures at distances of 50 meters or more. Finally, high-definition cameras often provide visual evidence of seep-associated benthic communities, offering a critical piece of information that guides the approach to seep sites.

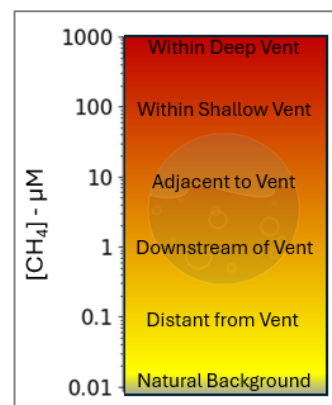


Figure 2. General methane concentrations in the vicinity of cold seeps; actual numbers vary widely.

Methane to Ethane Ratio from Seeps

The inclusion of a UMS offers unique opportunities. Once a hydrocarbon source is identified with the UMS, there is typically a sufficiently high methane signal during the approach to suspected seep sites allowing for the calculation of a C_1/C_2 ratio. If C_2 is absent, the instrument's detection limit can be used to determine the 'minimum' C_1/C_2 value for the hydrocarbon plume - still a useful metric. This method enables rapid, real-time identification of seep hydrocarbons that are likely biogenic or thermogenic in origin. Hydrocarbons with a C_1/C_2 ratio of less than 50 are considered high-confidence thermogenic, whereas ratios greater than 1000 suggest a biogenic source. Hydrocarbon plumes with C_1/C_2 ratios between 50 and 1000 suggest mixing or other complex relationships that warrant sample collection and isotopic analysis. Approaching seeps close enough for direct sampling can be time-consuming; if the C_1/C_2 ratio does not justify further exploration, the survey team may decide to proceed to the next site based on budgetary constraints.

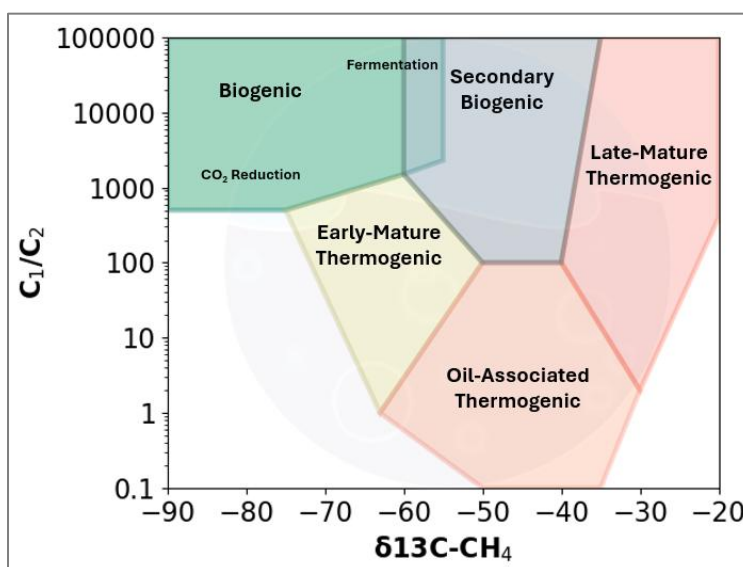


Figure 3. Bernard diagram enables classification of hydrocarbon sources; adapted from various sources⁸⁻¹¹.

The real-time *in situ* chemical data from the UMS can be used to trigger sample collection guaranteeing retrieval of a sample containing sufficient hydrocarbons for complete isotopic analysis. Furthermore, the chemical maps and visual seep identification allow this data to be positively and reliably correlated with specific seep sites – all without the need to take the time to approach the seep directly. To this end, Beaver Creek Analytical offers shipboard isotopic analysis of dissolved hydrocarbons to provide near-real-time results that enable the vessel to engage in adaptive, regional sampling strategies.

If the deployment platform has sufficient control (e.g., ROV), the seep might be approached even closer, enabling the detection of even higher concentrations of hydrocarbons. Real-time qualitative identification of compounds like propane, butane, pentane, cyclopentane, hexane, cyclohexane, heptane, benzene, and toluene would not be unexpected upon directly approaching bubbles from a seep emitting oil-associated thermogenic gases (Figure 4). By approaching the seep directly, there is further opportunity to directly sample bubbles and quantify their emission rate; visually identify seep-related benthic communities, carbonates, brines, mud-flows, and tar; or collect sediment cores in the area.

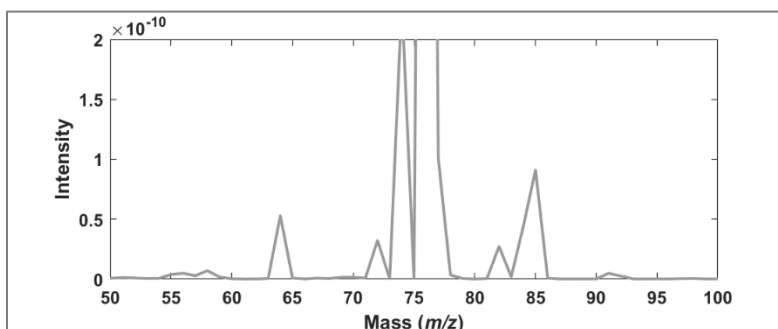


Figure 4. Underwater Mass Spectrum of degraded crude oil containing various light-hydrocarbons.

The real-time data produced by the UMS may identify multiple methane gradients near seep sites (Figure 5). This phenomenon is often the result of complex currents in a three-dimensional environment or the presence of multiple seeps within a single area sharing the same source reservoir, which is not unusual. However, different seep sources can coexist within one region, each with distinct characteristics stemming from varied origins⁸. For instance, mud volcanoes generally exhibit high C_1/C_2 ratios compared to oil-associated seeps, even though they are linked to shared geological features¹². As a result, seeps originating from mud volcanoes frequently show significantly different C_1/C_2 ratios compared to others in the region. In addition to H_2S , He , N_2 and CO_2 ^{13,14} containing seeps, these differences are quickly identified by the UMS during area survey.

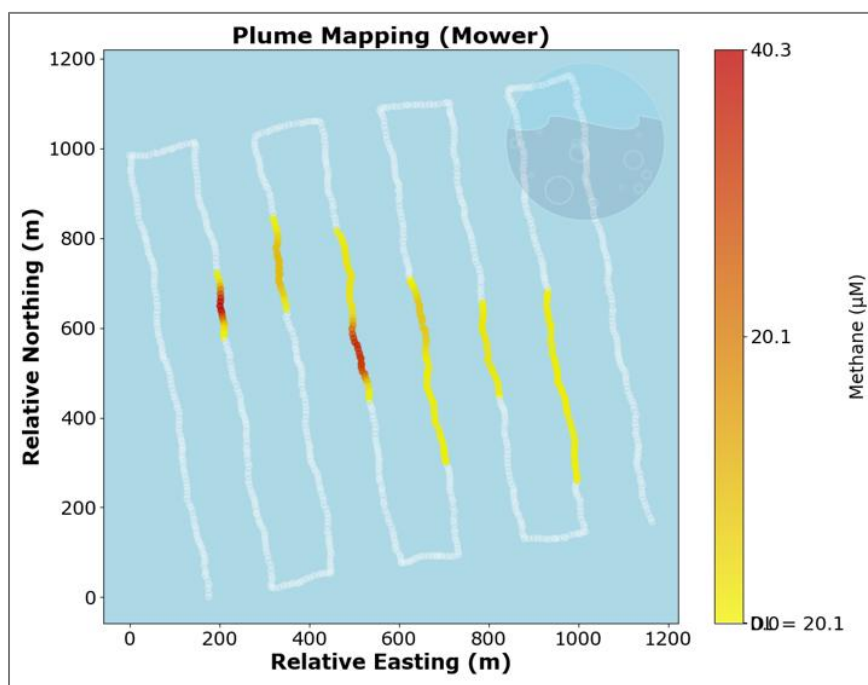


Figure 5. Simulated UMS data demonstrates complex chemical gradients in the vicinity of a simulated seep field.

Figure 6 illustrates the same *in situ* methane data as Figure 5 but includes mapped markers indicating the real-time determined C_1/C_2 ratios and their associated source classifications (see online version for interactive content at www.bcanalytical.com/seep-characterization). Utilizing this ethane data to inform the UMS allows users to ascertain the likely geological source of the seeps (biogenic versus thermogenic) before directly approaching them and facilitates the identification of multiple seep sources using general survey data despite their proximity.

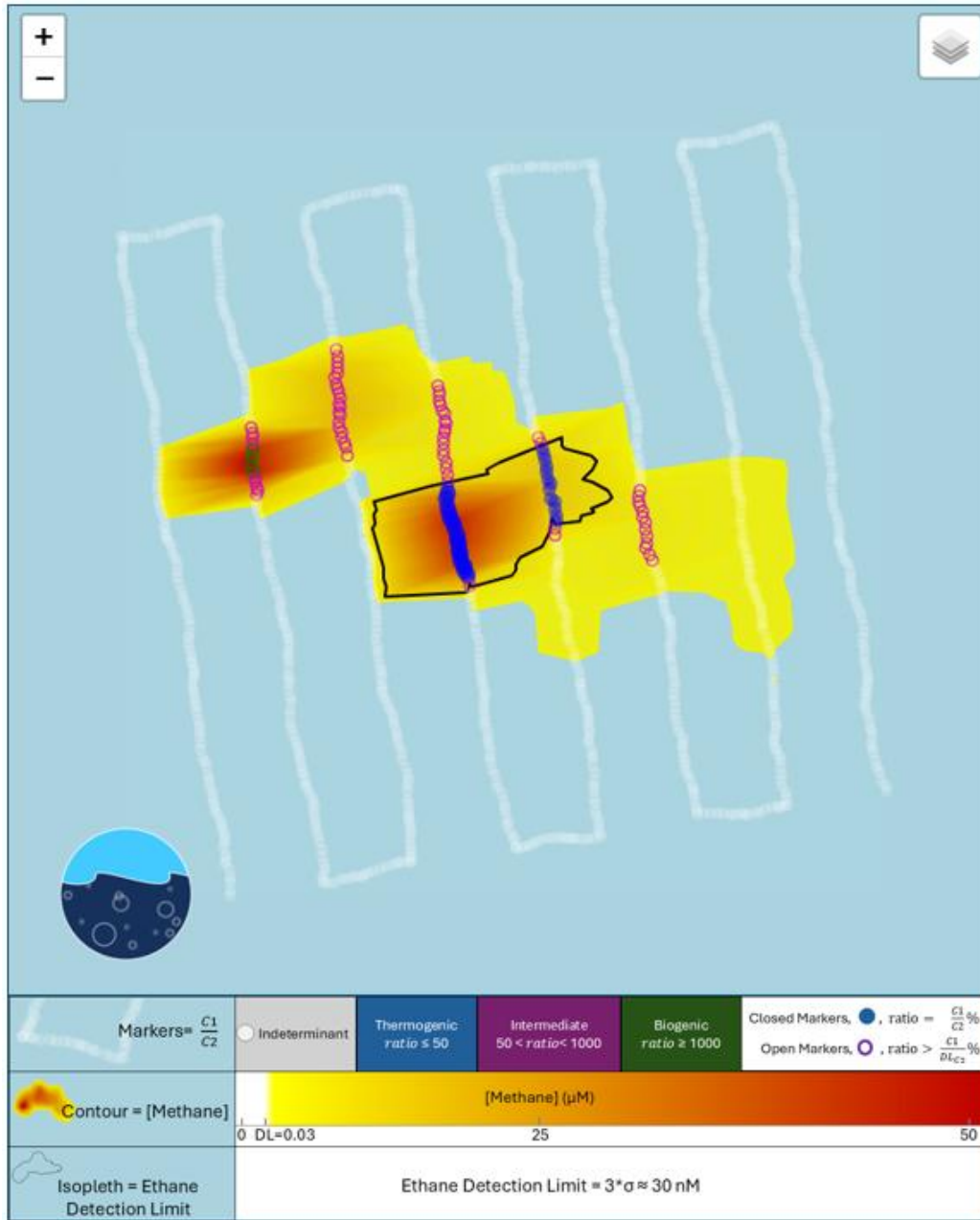


Figure 6. Simulated UMS data demonstrating the classification of seep hydrocarbons during a field survey. In this case, two seeps of disparate source reservoirs are identified.

Bubble vs Dissolved Gas Composition

Lastly, it is important to understand the relationship between bubble composition and the subsequent dissolved gas composition. As bubbles migrate over hundreds of meters, hydrocarbons diffuse into seawater while some dissolved atmospheric gases evaporate in the opposite direction, into the rising bubble. By the time a bubble reaches altitudes greater than 100 meters, if it still exists, its composition will have changed significantly¹⁵. Hydrostatic pressure will force continuous dissolution of a bubble, and a rising bubble will be constantly exposed to fresh water, meaning the rate of dissolution will be influenced by both diffusion rates and solubility coefficient (among other things). Methane and

ethane, having similar solubility and diffusion rates, will have a similar molar ratio in the dissolved aqueous fraction as the gaseous fraction still in the bubble.

That said, there is a tendency for methane transport into solution to be faster than ethane¹⁷ and for the dissolution transport of a bubble to be highest at the location of ebullition. As a result, dissolved gas determinations of molar C_1/C_2 obtained near a seep are predicted to be higher than the molar ratio within the bubble. Results from a TAMOC simulation¹⁶ of a single bubble rising from 600 m demonstrates the effect in Figure 7. As the bubble rises and gaseous methane is depleted relative to ethane, resulting in dissolved gas determinations of C_1/C_2 ratios that tend to be lower than the initial bubble composition. Of course, the dissolution process is very complex and is further affected by oceanic currents, vent jet-flow, oil-films, liquid-oil droplets, hydrate-films, films of naturally occurring surfactants.

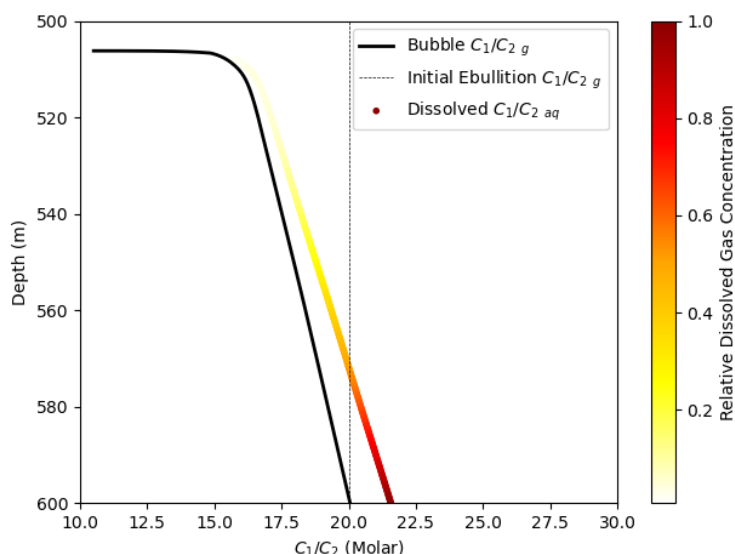


Figure 7. A TAMOC dissolution simulation of a single, clean, bubble from a 600 m vent in a simple immobile water column. The initial C_1/C_2 ratio was 20 (dashed line), C_1/C_2 ratio in the gaseous bubble (black line) shows complete dissolution at about 505 m. The resulting dissolved C_1/C_2 ratio (white-red colored line), indicates a relative methane enrichment at the location of bubble ebullition, and depletion high above. The color of this line indicates expected relative concentration resulting from this single bubble.

References

- (1) Abrams, M. A. Significance of Hydrocarbon Seepage Relative to Petroleum Generation and Entrapment. *Mar. Pet. Geol.* **2005**, 22 (4), 457–477. <https://doi.org/10.1016/j.marpetgeo.2004.08.003>.
- (2) Abrams, M. A. Evaluation of Near-Surface Gases in Marine Sediments to Assess Subsurface Petroleum Gas Generation and Entrapment. *Geosciences* **2017**, 7 (2), 35. <https://doi.org/10.3390/geosciences7020035>.
- (3) Hwang, J.; Bose, N.; Fan, S. AUV Adaptive Sampling Methods: A Review. *Appl. Sci.* **2019**, 9 (15), 3145. <https://doi.org/10.3390/app9153145>.
- (4) Dølven, K. O.; Ferré, B.; Silyakova, A.; Jansson, P.; Linke, P.; Moser, M. Autonomous Methane Seep Site Monitoring Offshore Western Svalbard: Hourly to Seasonal Variability and Associated Oceanographic Parameters. *Ocean Sci.* **2022**, 18 (1), 233–254. <https://doi.org/10.5194/os-18-233-2022>.

- (5) Fu, L.; Liu, Y.; Wang, M.; Lian, C.; Cao, L.; Wang, W.; Sun, Y.; Wang, N.; Li, C. The Diversification and Potential Function of Microbiome in Sediment-Water Interface of Methane Seeps in South China Sea. *Front. Microbiol.* **2024**, *15*, 1287147. <https://doi.org/10.3389/fmicb.2024.1287147>.
- (6) Gentz, T. Distribution and Fate of Methane Released from Submarine Sources – Results of Measurements Using an Improved in Situ Mass Spectrometer. phd, University of Bremen, 2013. <http://epic.awi.de/33993/> (accessed 2014-01-21).
- (7) Yapa, P. D.; Dasanayaka, L. K.; Bandara, U. C.; Nakata, K. A Model to Simulate the Transport and Fate of Gas and Hydrates Released in Deepwater. *J. Hydraul. Res.* **2010**, *48* (5), 559–572. <https://doi.org/10.1080/00221686.2010.507010>.
- (8) Bernard, B. B.; Brooks, J. M.; Sackett, W. M. Natural Gas Seepage in the Gulf of Mexico. *Earth Planet. Sci. Lett.* **1976**, *31* (1), 48–54. [https://doi.org/10.1016/0012-821X\(76\)90095-9](https://doi.org/10.1016/0012-821X(76)90095-9).
- (9) Whiticar, M. J. Carbon and Hydrogen Isotope Systematics of Bacterial Formation and Oxidation of Methane. *Chem. Geol.* **1999**, *161* (1), 291–314. [https://doi.org/10.1016/S0009-2541\(99\)00092-3](https://doi.org/10.1016/S0009-2541(99)00092-3).
- (10) Tazaz, A. M.; Bebout, B. M.; Kelley, C. A.; Poole, J.; Chanton, J. P. Redefining the Isotopic Boundaries of Biogenic Methane: Methane from Endoevaporites. *Icarus* **2013**, *224* (2), 268–275. <https://doi.org/10.1016/j.icarus.2012.06.008>.
- (11) Milkov, A. V.; Etiope, G. Revised Genetic Diagrams for Natural Gases Based on a Global Dataset of >20,000 Samples. *Org. Geochem.* **2018**, *125*, 109–120. <https://doi.org/10.1016/j.orggeochem.2018.09.002>.
- (12) Etiope, G.; Feyzullayev, A.; Baci, C. L. Terrestrial Methane Seeps and Mud Volcanoes: A Global Perspective of Gas Origin. *Mar. Pet. Geol.* **2009**, *26* (3), 333–344. <https://doi.org/10.1016/j.marpetgeo.2008.03.001>.
- (13) McGinnis, D. F.; Schmidt, M.; DelSontro, T.; Themann, S.; Rovelli, L.; Reitz, A.; Linke, P. Discovery of a Natural CO₂ Seep in the German North Sea: Implications for Shallow Dissolved Gas and Seep Detection. *J. Geophys. Res. Oceans* **2011**, *116* (C3). <https://doi.org/10.1029/2010JC006557>.
- (14) Etiope, G. *Natural Gas Seepage: The Earth's Hydrocarbon Degassing*; Springer International Publishing: Cham, 2015. <https://doi.org/10.1007/978-3-319-14601-0>.
- (15) McGinnis, D. F.; Greinert, J.; Artemov, Y.; Beaubien, S. E.; Wüest, A. Fate of Rising Methane Bubbles in Stratified Waters: How Much Methane Reaches the Atmosphere? *J. Geophys. Res. Oceans* **2006**, *111* (C9). <https://doi.org/10.1029/2005JC003183>.
- (16) Socolofsky, S. A.; Dissanayake, A. L.; Jun, I.; Gros, J.; Arey, J. S.; Reddy, C. M. Texas A&M Oilspill Calculator (TAMOC): Modeling Suite for Subsea Spills; 2015.
- (17) Gros, J.; Arey, J. S.; Socolofsky, S. A.; Dissanayake, A. L. Dynamics of Live Oil Droplets and Natural Gas Bubbles in Deep Water. *Environ. Sci. Technol.* **2020**, *54* (19), 11865–11875. <https://doi.org/10.1021/acs.est.9b06242>.